Advances in modelling the ECT of U-bend steam generator tubes based on the boundary element method

Edouard Demaldent, Christophe Reboud, Frédéric Nozais, Thierry Sollier, Cattiaux Gérard

Advances in Modelling the ECT of U-Bend Steam Generator Tubes Based on the Boundary Element Method

Edouard DEMALDENT[a,1], Christophe REBOUD[a], Frédéric NOZAIS[a],
Thierry SOLLIER[b] and Gérard CATTIAUX[b]
[a] *CEA, LIST, Saclay, 91191 Gif-sur-Yvette, France*
[b] *IRSN, Fontenay-aux-Roses, France*

Abstract. The modelling of the eddy current testing of U-bend steam generator tubes is a valuable tool for interpreting measured signals due to geometric distortions that can arise during the bending process. Especially, the decentred trajectory of the probe into the bending must be taken into account to ensure the accuracy of the simulated signal. As the exact trajectory is a priori not known, we propose an efficient way to build a database of the simulated signal for all possible positions of the probe into the tube, based on an adaptation of the boundary element method that is developed at CEA LIST.

Keywords. Eddy Current Testing, Modelling, Boundary Element Method

1. Motivation

We are interested in modelling the eddy current testing (ECT) of U-bend tubes in steam generators that are part of the second barrier containment of radioactive materials in nuclear pressurized water reactors. In addition to the curvature of the tube, whose modelling has already been successfully achieved for example in [1] and recently used in [2] in complex configurations, the bending process may cause a variation in thickness as well as the distortion of the inner wall of the tube [3-5]. It also affects the movement of the probe that is shifted and may be tilted in the bending. The detection and characterization of defects in this zone requires a signal analysis due to these phenomena and thus their modelling. Numerical simulation is challenging as the method used must be sufficiently flexible to adjust to small geometric distortions and accurate enough so as the digital noise does not disturb their low signal variations. As part of a collaboration between CEA LIST and IRSN that is, the French public expert in nuclear and radiological risks, we use an integral formulation [6] handled by the boundary element method (BEM) [7-9] to simulate the effects of the bending for ECT.

[1] Corresponding Author, E-mail: edouard.demaldent@cea.fr

A synthetic description of the BEM and of its specific use for this study are given in sections 2.1 and 2.2, respectively. Recently, these numerical tools made it possible to observe the sensitivity of the probe response to its trajectory in the bending [10].

A numerical assistance strategy for determining this trajectory is therefore proposed in section 3.1. It is based upon the use of a database of coil impedance variation for all mechanically admissible positions of the probe in the bending. The main originality of this contribution lies in this modelling strategy which is made viable thanks to the previously introduced BEM. An X-ray imaging of the probe in the bending revealed the distortion of the inspected tube as well as the effective position of the probe and validates, yet partially, the proposed strategy in section 3.2.

Once the probe location is established, the ECT response of a defect can be simulated, allowing to observe the effect of the bending onto its signature. Section 4 shows that this perturbation remains secondary by comparison with the trajectory of the bobbin coil.

2. Advanced Boundary Element Method

2.1. Boundary Element Method

The 3D problem can be expressed as an equivalent transmission problem at the interface between homogeneous parts of the medium by a suitable integral representation form [6]. The goal then becomes to compute the electric (J = n x H) and magnetic (M = E x n) surface current densities (n stands for the normal at the interface, E and H are the electric and magnetic fields). A Galerkin discretization of the variational form then enables us to approximate the physical solution by solving a linear system.

Compared to the finite element method, the number of unknowns within the boundary element method is dramatically reduced (but the matrix is full with complex filling) and therefore the use of a direct solver becomes possible. A direct solver is far more effective than an iterative one when we face a system that is ill-conditioned or presenting many RHS (right hand sides), provided that the number of unknowns remains limited (a few tens of thousands). Hence it is generally well suited to ECT applications for which we can count thousands of RHS (positions of the coil) in a restricted computational domain, due to the localized support of the source and to negligible propagation effects.

A higher-order approximation [7] (i.e. increasing the polynomial degree of the expansion) further reduces the number of unknowns for a given precision, therefore making more accessible the direct solver. In practical terms, the increase of the order of the mesh allows the use of a small number of surface elements with curved edges that are particularly effective for modelling smooth geometric distortions.

2.2. Adapted BEM

Such a high order boundary element method is currently implemented at CEA LIST. Firstly developed for magneto-static applications such as the modelling of 3D ferrite cores [11], this approach has been expanded to low frequency electromagnetic applications [8] and especially to the quasi-static eddy current regime [9]. In what follows as in [12] we use Hdiv-conforming boundary elements similar to [7] with a quasi-

Helmholtz decomposition (see e.g. [13]) of the integral boundary formulation presented in [8] without the multi-step option.

The quality of the discrete mesh is crucial as low changes of the curvature may lead to high numerical noise with regards to the slight variations of signal we are looking for. As a first step, meshing is performed on a portion of the straight tube for nominal parameters (external diameter of 19.05 mm, thickness of 1.09 mm and conductivity of 1 MS/m). This mesh is composed of quadrilateral elements with curved edges, whose size increases as the element is closer from the truncation. Then, for a given axial location of the probe in the bending, corresponding distortions are applied to the straight mesh to obtain the deformed one (Figure 1). Finally the probe is shifted and tilted as wanted.

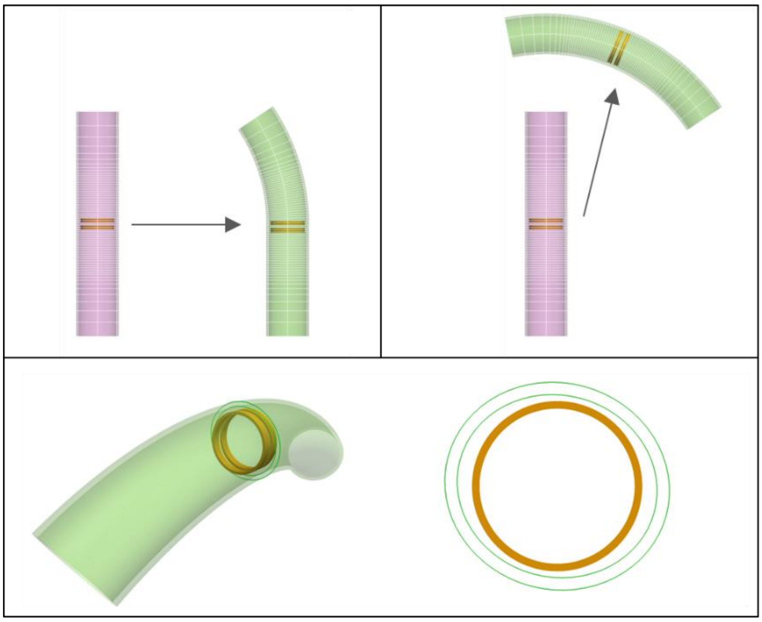

Figure 1. Mesh of the straight (purple) and of the deformed (green) SG tubes for two locations of the probe (orange), considering an ovalization and a torsion (bottom).

The small number of high-order basis functions (here 2 × 7424 1st and 2nd mixed-order basis functions) allows us to use a LU-based direct solver, so that many tilt and shift variations can be treated in a single calculation at a fixed axial position of the probe. This has facilitated the achievement of parametric studies to identify the most influent inputs, namely the distortion (such as ovalization) of the inner tube wall and the probe path for a bobbin coil [10]. As a matter of fact, these parameters vary depending on the tubes and the probes and are not explicitly known.

3. Proposed Strategy

3.1. Simulation tools to help determine the path of the probe

We therefore focused on a simulation strategy that can assist NDT practitioners in describing the probe position. This strategy first consists in generating (by forward simulation) a database of the coil impedance variation of all the mechanically admissible positions of the probe in the tube.

The plastic body of the probe is first introduced into the geometric model. Shown in Figure 2.1, this body is represented by a cylinder whose ends are two half ellipses. The envelope of the mechanically possible positions is then determined by a landing algorithm of this probe body onto the inner wall of the mesh. Illustrated in Figure 2.2 for a fixed axial position, this (2D) section of the (3D) envelope is read from bottom to top for the shift and from left to right for the tilt. The signal is then calculated on a representative basis. This is illustrated Figure 2.3 on a complete tube for which we consider here a gradual ovalization from the straight part to the top of the bending (the tip), with a sensor operated in absolute mode. These impedance variations are not calibrated and are given for information purposes only.

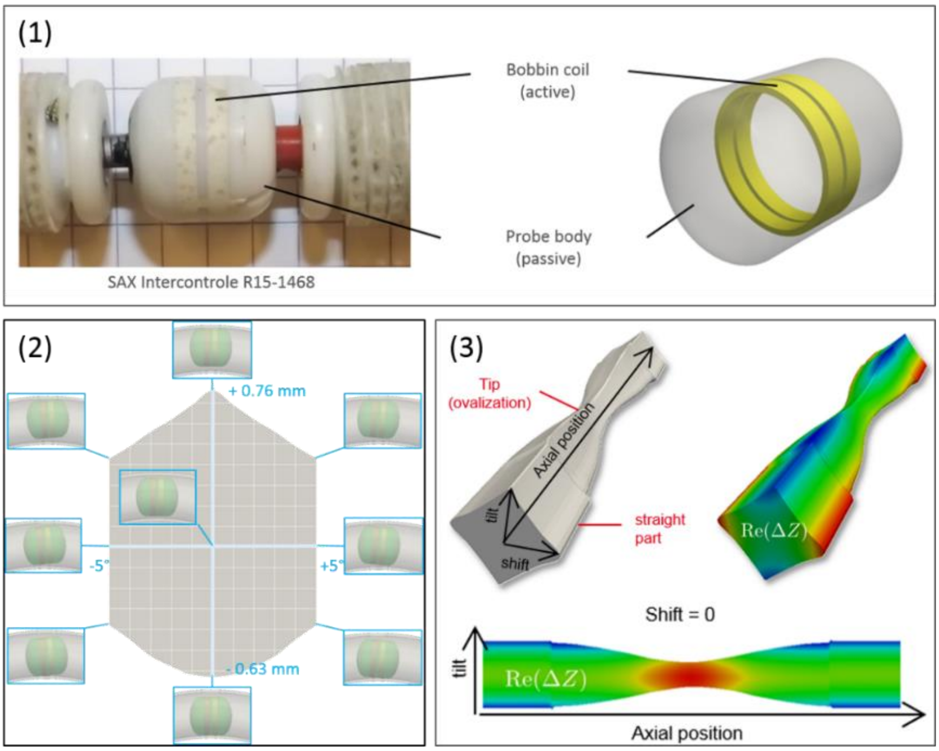

Figure 2. Geometric modelling of the plastic body of the probe (1), 2D envelope of the admissible positions of the probe at a given axial position in the bending (2), 3D envelope for the complete U-bend tube and corresponding impedance variation of the signal (3).

Realized as a pre-processing step (offline), building such a databases requires 1 to 2 hours of calculation on a standard PC. This computation time is directly related to the deformation profile of the tube: fast deformations with regards to the axial displacement of the probe would necessitate increasing the number of forward unit simulations (i.e. fixed axial positions) and would therefore generate an additional cost of the order of the hour.

Once this database is available, the second step would be to simulate (on line) the impedance variation signal for a large number of parametric trajectories of the probe and to rely on acquisitions to refine this parametrization. However such a parametrization should be based on few trajectory observations that are hardly available. An alternative could be to estimate the trajectory using Kalman filter.

3.2. Adjustment of geometric parameters through X-ray inspection for validation

X-ray imaging of probe was performed at the top of the bending to set the geometric inputs of the model (Figure 3.1 and Figure 4.1). Figure 4.1, inside the tube, the red lines delimit the boundary of the coils (external diameter of 14.36 mm, thickness of 0.67 mm) while the green line corresponds to the boundary of the plastic body of the probe (diameter of 15.00 mm). Onto the tube, red and blue lines correspond to outer and inner walls of the tube while dashed black lines correspond to a perfect cylinder (the tube with no distortion).

These inputs were taken into account in the model (Figure 4.2) and the signal was simulated for each inspection channel on the envelope of the mechanically possible positions of the probe at this axial position (Figure 4.3). Each result has then be restricted to the zone where the simulated signal is close to the acquisition (Figure 3.2). The intersection of the resulting reduced envelopes indicates the supposed position of the probe, here in contact with the extrados (Figure 4.4).

Incorrect results (shifted probe towards the intrados) were obtained before imaging, when simulating the signal on a U-bend tube with no distortion [10]. This sensitivity would justify extending the database to the main geometrical distortion inputs.

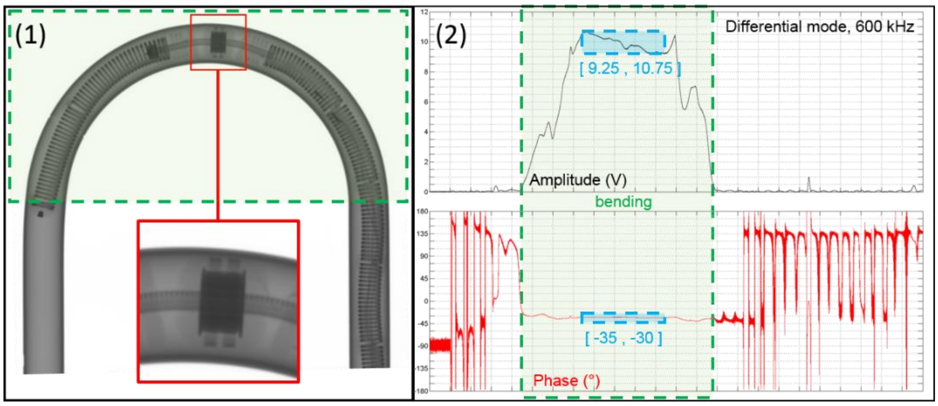

Figure 3. X-ray imaging of the probe at the tip (1) and experimental measurement for a probe operated in absolute mode at 600 kHz (2).

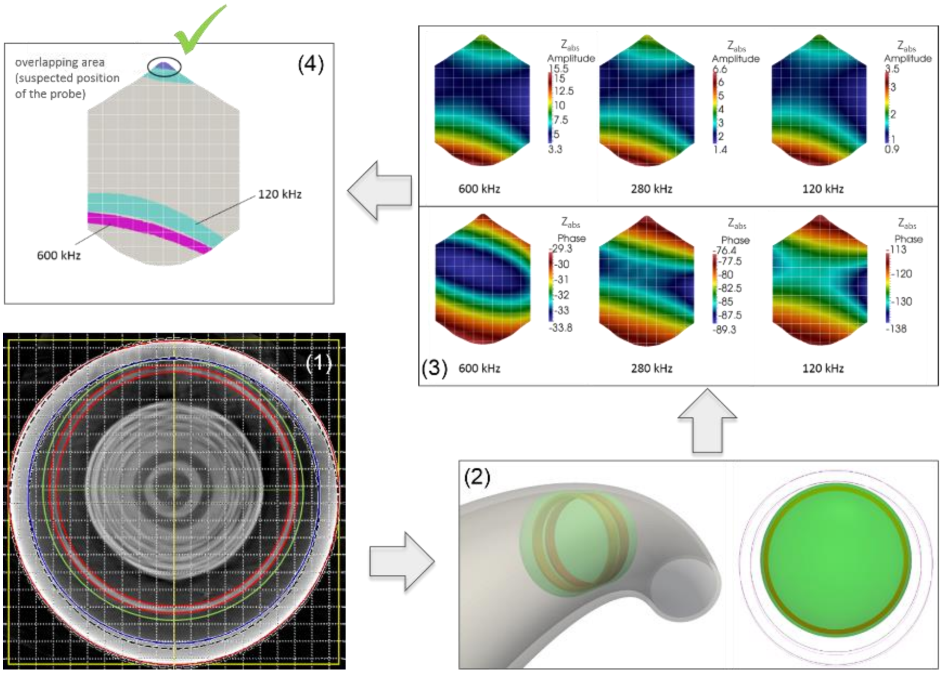

Figure 4. X-ray imaging of the probe at the top of the bending (1), corresponding geometric modelling (2), phase and amplitude of the simulated signal for the admissible positions of the probe (here operated in absolute mode) (3), and intersection of the reduced envelopes (4).

4. Simulation of the defect's signature

Standard defects such as grooves & notches were introduced in the straight tube, before distortion. Hence their effective depth is not absolute but relative to the local thickness of the section. This process and the few simulated defects are illustrated Figure 5.

Simulations were carried out for a straight tube then for a 3-inch bending, with a shifted probe at 200 µm or in contact with the extrados (lift-off = 0 mm), as well as for a centred probe in the straight tube. The defect signals were balanced (but not calibrated) with the defect-free signal for a corresponding probe position so as to focus on the possible correlation between the flaw response and the geometry signal.

It is found that the simulated signals vary only slightly with the bending, with at most a phase shift of a few degrees compared with the signals obtained in the straight part of the tube for the same probe shift, as shown in Figure 6. Taking into account the tube wall distortion revealed by X-ray imaging did not alter this observation on the few defects studied.

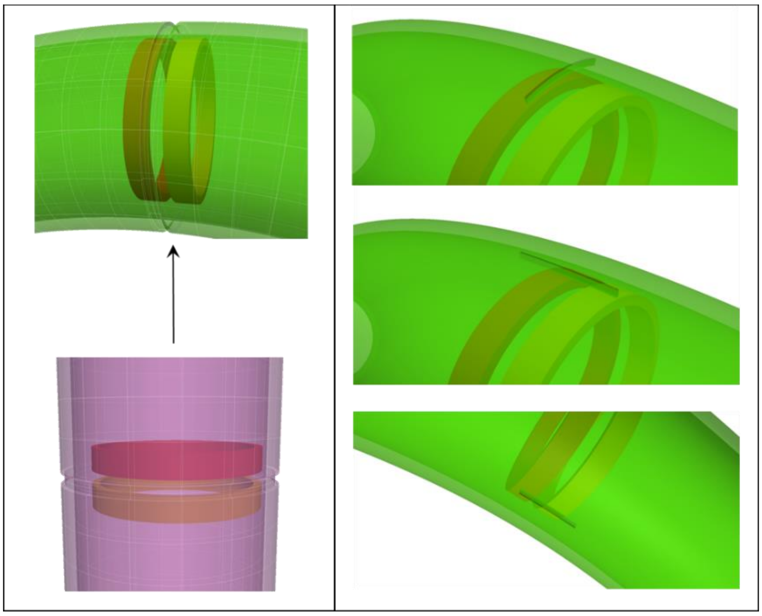

Figure 5. Geometric modelling of simple defects.

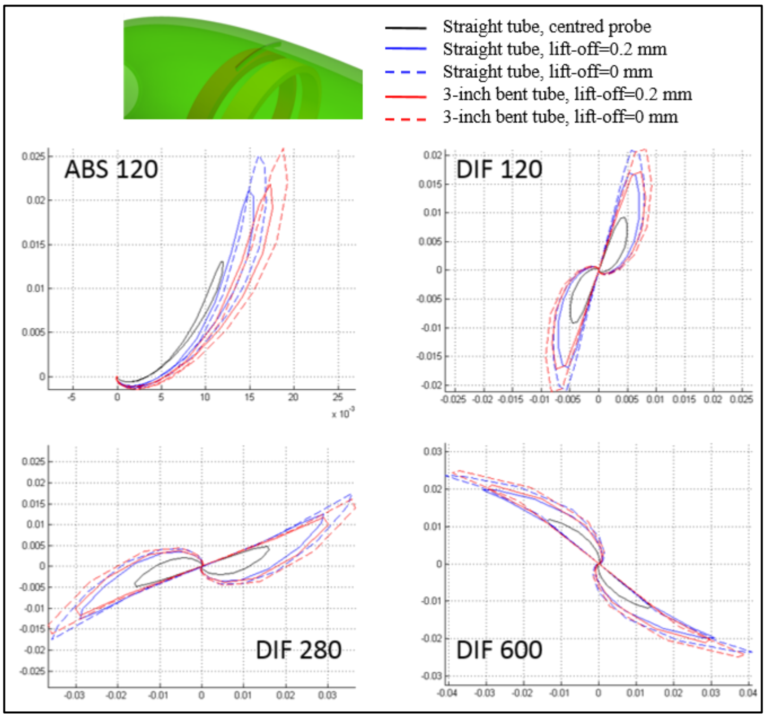

Figure 6. Simulation of the ECT signal with a circumferential notch (40% depth, 6 mm x 0.15 mm) and two bobbin coils operated in absolute mode (ABS) at 120 kHz and differential mode (DIF) at 120, 280, 600 kHz.

5. Conclusion

Modelling the eddy current testing in the bending of a steam generator tube requires good knowledge of the probe's trajectory. Since this trajectory is not known explicitly, we proposed simulation tools to assist its parametrization.

Based on the use of a database for which direct calculations are carried out using a higher-order boundary element method, this process has been partially validated by experimental measurements carried out in the framework of this study. It is found that the process is particularly sensitive to the tube wall deformation, suggesting that the database should be extended to the principal distortion inputs.

On the other hand, first simulations tend to show that the response of a defect is very sensitive to the trajectory of the bobbin coils but remains relatively insensitive to the deformation of the tube. This should motivate the search for a post-treatment of (fast) simulations made on a simplified geometry. More precautions should be taken with pancake coils, and additional geometric effects such as pilger noise should be investigated to complete and confirm these observations.

References

[1] O. Mihalache, T. Yamaguchi and M. Ueda, Large scale 3D FEM Electromagnetic simulations and validations for FBR steam generator tubes, Electromagnetic Nondestructive Evaluation (XVI), vol. 38, pp. 94-102, 2013.

[2] O. Mihalache, T. Yamaguchi, T. Shirahama and M. Ueda, R&D of multi-frequency ECT algorithms for FBR SG tubes, E-Journal of Advanced Maintenance, vol. 9-2, pp. 60-65, 2017.

[3] D. Diercks, W. Shack and J. Muscara, Overview of steam generator tube degradation and integrity issues, *Nuclear Engineering and Design,* vol. 194, n° 11, pp. 19-30, 1999.

[4] W. Cheng and I. Finnie, Stress analysis and fatighe life prediction for a U-bend steam generator tube, *Nuclear Engineering and Design,* vol. 165, n° 11-2, pp. 101-109, 1996.

[5] S. Bakhtiari, C. Bahn and T. W. Elmer, Inspection reliability assesments associated with steam generator tube U-bend degradations, *31th annual EPRI Steam Generator NDE Workshop*, Bretton Woods, New Hampshire, USA, 2012.

[6] J.-C. Nédélec, Acoustic and electromagnetic equations: integral representations for harmonic problems, Springer, 2001.

[7] R. D. Graglia, D. R. Wilton and A. F. Peterson, Higher order interpolatory bases for computational electromagnetics, *IEEE Transactions on Antennas and Propagation*, vol. 45, n°3, pp. 329-342, 1997.

[8] A. Vigneron, E. Demaldent and M. Bonnet, A multi-step solution algorithm for Maxwell boundary integral equations applied to low frequency elctromagnetic testing of conductive objects, *IEEE Transactions on Magnetics,* vol. 52, 2016.

[9] M. Bonnet, E. Demaldent and A. Vigneron, Asymptotic Expansion of the Maxwell Integral Equation Formulation Applied to Eddy Current Testing, *22th International Workshop on Electromagnetic Nondestructive Evaluation*, Saclay, France, 2017

[10] E. Demaldent, C. Reboud, J.-M. Decitre, T. Sollier and G. Cattiaux, Modelling the ECT of U-bend steam generator tubes by the boundary element method, *19th World Conference on Non Destructive Testing*, Munich, Germany, 2016.

[11] E. Demaldent, C. Reboud, T. Sollier and G. Cattiaux, Efficient simulation of steam generator tubes inspection with the Pluspoint eddy current probe, *11th European Conference on Non-Destructive Testing (ECNDT)*, Pragues, 2014.

[12] E. Demaldent, R. Miorelli, M. Reboud and T. Theodoulidis, Solution of the WFNDEC 2015 eddy current benchmark with surface integral equation, AIP Conference Proceedings, vol. 1706, p. 190002, 2016.

[13] F. Valdès and F. Andriulli, High-order div- and quasi curl-conforming basis functions for Calderón multiplicative preconditioning of the EFIE, IEEE Transactions on Antennas and Propagation, vol. 59, no. 4, 2011.